Materials Science in Semiconductor Processing xxx (xxxx) xxx

Contents lists available at ScienceDirect

Materials Science in Semiconductor Processing

journal homepage: http://www.elsevier.com/locate/mssp

# Effect of oxygen concentration on minority carrier lifetime at the bottom of quasi-single crystalline silicon

Chunlai Huang [a,b], Peng Wu [b], Lei Wang [a,*], Deren Yang [a,**]

[a] State Key Lab of Silicon Materials and Department of Materials Science & Engineering, Zhejiang University, Hangzhou, 310027, China
[b] Jiangsu Key Lab of Silicon Based Electronic Materials, Jiangsu GCL Silicon Material Technology Development Co., Ltd., No.88 Yangshan Road, Xuzhou Economic Development Zone, Xuzhou, 221000, China

ARTICLE INFO

*Keywords:*
Casting silicon
Minority carrier lifetime
Oxygen concentration
Red zone

ABSTRACT

The formation mechanism of red zone in casting silicon ingots was investigated. Oxygen and metal distribution in ingots of crystalline Si were determined and analyzed. It was found that metal impurities is not the only factor to form bottom low minority carrier lifetime region. Interstitial oxygen with relative high concentration also decreases carrier lifetime at ingot bottom.

## 1. Introduction

With awareness about global warming increasing and given the ongoing crisis related to the use of fossil fuels, the photovoltaic (PV) industry has been growing rapidly in recent years. Czochralski Si (Cz-Si) and casting multicrystalline Si (mc-Si) are the primary substrate materials in PV devices, with a market share of more than 90%. The advantages of mc-Si include low cost, high throughput and feasibility for production. However, the material quality of mc-Si is poorer compared to Cz-Si, because of the presence of randomly oriented grains and multiple structural defects. As a result, the conversion efficiency of solar cells based on mc-Si is usually 1–2% lower than that of cells based on Cz-Si [1]. In the past decade, the idea and techniques of quasi single crystalline silicon (QSC-Si) [2] became a trend in casting silicon. The advantages of QSC-Si compared to mc-Si are single orientation and lower grain boundary content. Therefore, QSC-Si has the great potential to be applied in PV industry. However, QSC-Si ingots usually exhibit a low carrier lifetime zone (lower than 2 μs) at the bottom, which is referred as "red zone" in PV industry. The red zone should be cut away before wafer cutting because they are not qualified for solar cell fabrication. In fact, this zone exists also in conventional mc-Si ingots. It is well known that minority carrier lifetime in mc-Si mainly determined by dislocation density, metal impurity, oxygen content [3–7]. The widely accepted mechanism for red zone formation is the diffusion of metal impurities from $Si_3N_4$-coated quartz crucible [8]. But the height of red zone in QSC-Si is obviously higher than that in conventional mc-Si due to the introduction of seeds, which introduces additional cost for QSC-Si fabrication. Therefore, the formation mechanism of red zone at the bottom of QSC-Si has attracted much attention. Later, seed-assisted mc-Si (high performance multicrystalline silicon, HPM-Si) became the main trend of mc-Si. The red zone height of HPM-Si is close to that of QSC-Si when the seed thickness is same. However, an interesting phenomenon is that high-purity crucible and coating cannot result in a significant reduction in the red zone height in QSC-Si ingots, although they can form a much shorter bottom red zone in conventional mc-Si ingots [9]. One explanation is that impurities in the liquid Si can diffuse back into the seeds during the seed preservation stage, and causes the contamination [10]. Another explanation suggested that the main factor is the metal diffusion from the iron-rich layer, which is formed during the initial solidification stage [11]. The iron-rich layer is crystallized from the transient layer at the solid/liquid interface, the iron concentration at which is high due to segregation under high growth rate [11]. These interpretations show that the formation mechanism of QSC-Si red zone remains controversy and unclear.

In this study, the formation mechanism of bottom red zone in QSC-Si ingots was investigated. Especially, the influence of interstitial oxygen at the bottom red zone was studied. It was found that although metal impurities are the main factor for reduced carrier lifetime, oxygen and its precipitates also reduce the carrier lifetime at ingot bottom.

* Corresponding author.
** Corresponding author.
*E-mail addresses:* phy_wangl@zju.edu.cn (L. Wang), mseyang@zju.edu.cn (D. Yang).

https://doi.org/10.1016/j.mssp.2020.105497
Received 1 August 2020; Received in revised form 29 September 2020; Accepted 6 October 2020

## 2. Experimental

Seed-assisted boron-doped mc-Si and QSC-Si ingots were produced using the directional solidification (DS) method. Si particle seeds and Cz-Si seeds were prepared for HPM-Si ingots and QSC-Si ingots, respectively. Seed-assisted growth required partially melted seeds, the heights of un-melt seeds for all ingots were controlled at ~15 mm. The solidification time for the ingots was approximately 27 h. Other physical properties of all ingots are: weight of ~850 kg, height of ~37 cm, and resistivity of 1.3–2.1 Ω·cm. Moreover, growth based on mc-Si and Cz-Si seeds were performed with regular $Si_3N_4$ coating and high-purity coating to elucidate the influence of metal contamination from crucibles. Four ingots were grown in total. After growth, the concentrations of metal impurities, interstitial oxygen of wafers at various regions was measured. And minority carrier lifetime mapping was measured to evaluate the crystal quality.

The minority carrier lifetimes were measured by the microwave photoconductivity decay (μ-PCD) method (Semilab, WT-2000). The concentration of interstitial oxygen was measured by Fourier transform infrared spectrometry (FTIR) system (IFS 66V/S) at room temperature. The test wafer was prepared by chemical polishing in an acid solution ($HNO_3$/HF = 3:1) for 1 min, and the final thickness was ~ 2 mm. The conversion coefficient of $3.14 \times 10^{17}$ $cm^{-2}$ (ASTM F121–89) was adopted. The concentration distributions of metal impurities were measured by inductively coupled plasma mass spectrometry (ICP-MS).

## 3. Results and discussion

Fig. 1 shows the minority carrier lifetime maps of the HPM-Si and QSC-Si ingots using regular $Si_3N_4$ coating. There are sizeable red zones at the bottom of both ingots, and the heights are nearly the same. However, for high-purity coating, the red zone height of HPM-Si ingot was decreased from ~60 mm to ~46 mm, while the height of QSC-Si ingot was almost unchanged (~60 mm), as shown in Fig. 2.

Fig. 3 shows the iron distributions at the bottom of the HPM-Si and QSC-Si ingots grown by using the crucible with regular or high-purity coating, which were measured by ICP-MS, corresponding to the total body concentration. Firstly, the adoption of high-purity coating effectively reduced the iron concentration for both HPM-Si and QSC-Si ingots, because this coating can suppress the diffusion from the crucible [9]. Note an interesting fact that the iron concentration in QSC-Si is slightly lower than in the HPM-Si, for both coatings, which does not fit the result in Fig. 2. The red zone height of QSC-Si with high-purity coating was not reduced. Since the reduction in iron concentration should increase the carrier lifetime and hence reduce the red zone height, which is true for the HPM-Si but false for the QSC-Si. Therefore, it can be reasonably inferred that there are factors on the bottom carrier lifetime for QSC-Si other than iron impurities.

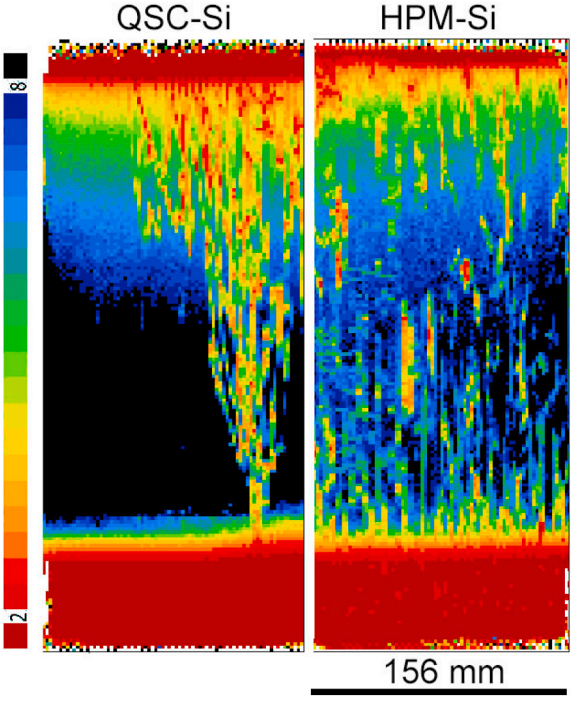


**Fig. 1.** Minority carrier lifetime maps of the cross-section of QSC-Si (left) and HPM-Si (right) ingots with the same seed height.

Fig. 4 shows the concentration of interstitial oxygen in the HPM-Si and QSC-Si ingots produced with high-purity coatings. The concentration of interstitial oxygen in both the ingots decreases along ingot height. And the oxygen concentration in the QSC-Si ingot was higher than that in the HPM-Si ingot. As mentioned in Fig. 2, the red zone heights of HPM-Si and QSC-Si ingots were ~46 mm and ~60 mm, respectively. Note that at the edge of QSC-Si red zone (~60 mm), the concentration of oxygen was $4.3 \times 10^{17}$ at/cm$^3$, while that at the same height for the HPM-Si red zone (~60 mm) was $3.8 \times 10^{17}$ at/cm$^3$. Through industrial production statistics, at the end of the crystal growth process, the temperature at the crucible bottom was approximately 1000 °C. It was found that the interstitial oxygen content at the edge of the bottom red zone of the ingots corresponded to the solubility in solid Si, which is $4.47 \times 10^{17}$ at/cm$^3$ [12,13]. Therefore, there might be more oxygen content here existing in the form of precipitates. Since the oxygen concentration at QSC-Si bottom is higher than at HPM-Si, it can be assumed that the difference in oxygen content can be the major factor for lifetime reduction in QSC-Si.

The relationship between oxygen content and red zone height was further investigated in multiple QSC-Si ingots. Fig. 5 shows the relationship between red zone height and interstitial oxygen content (at 45 mm height). The tested ingots have the same residual height of seed, and the interstitial oxygen content can be modified by adjusting the convection of the melted silicon. Interestingly, when the interstitial oxygen content was lower than $4 \times 10^{17}$ at/cm$^3$, the red zone height was ~47 mm. When the interstitial oxygen content was above $4 \times 10^{17}$ at/cm$^3$, the red zone height increased with the interstitial oxygen content. These results suggest that for these QSC-Si, interstitial oxygen content has strong positive correlation with the red zone height when the content is higher than $4 \times 10^{17}$ at/cm$^3$, which is very likely to be caused by the formation of oxygen precipitates because the threshold is very close to the solubility of interstitial oxygen.

In total, the results described so far would suggest that the bottom red zone was caused by both metal and oxygen impurities. As the segregation coefficient of metal atoms is lower than $10^{-4}$, the metal impurities are primarily distributed in the head of the ingots, with those at the bottom of the ingots being attributable to the crucible or the remaining seed layer. It was previously reported [9] that the diffusion distance of iron atoms is less than 3 cm from the crucible or the remaining seed at 1100 °C. During the melting process, the temperature near the seed is lower so that its melting is prevented. The surface of the polycrystalline-Si melts first, so that the oxygen concentration in this area is higher. The liquid Si solidifies epitaxially at the Si seed. During the final stage of the melting process, this Si material and the residual seed both remelt. As the temperature near the seed is lower, an inversion or laminar layer of a certain thickness forms above it. The thermal convection of the liquid Si in the laminar layer is very faint. Thus, a high-oxygen-content layer of molten Si could be formed above the residual seed. As the growth process progresses, the concentration of the interstitial oxygen in the red zone might become higher than the oxygen solubility. As a result, more oxygen precipitates could be nucleated at the bottom of the Si ingot. It is known that carrier recombination at strained oxide precipitates is stronger and is dependent on the density of the precipitates instead of their size [7]. This is very likely to be the reason why the minority carrier lifetime at the QSC-Si bottom of the

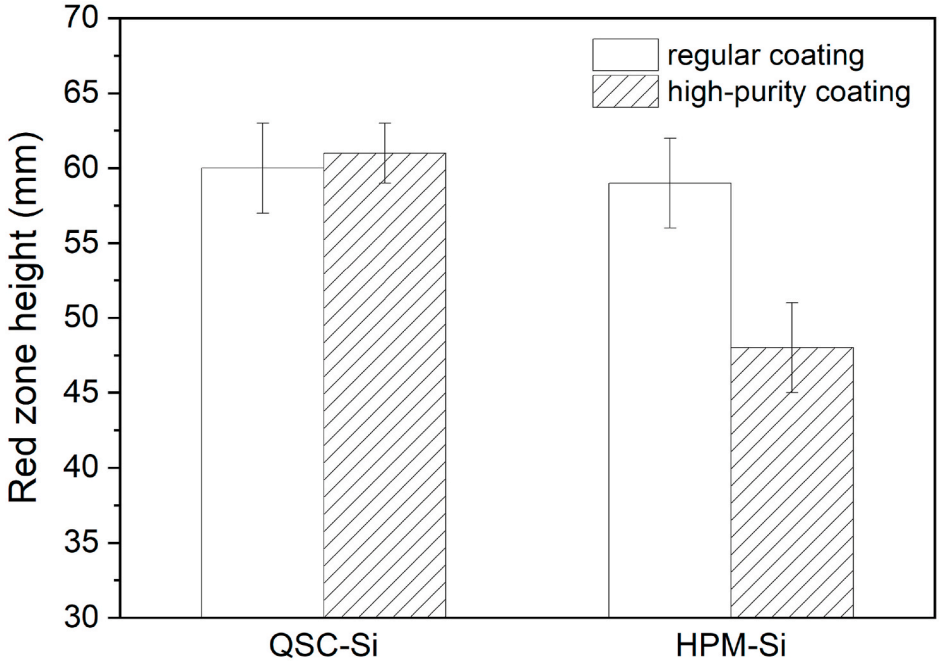


**Fig. 2.** Height of bottom red zones of QSC-Si and HPM-Si ingots using regular or high-purity coating, respectively.

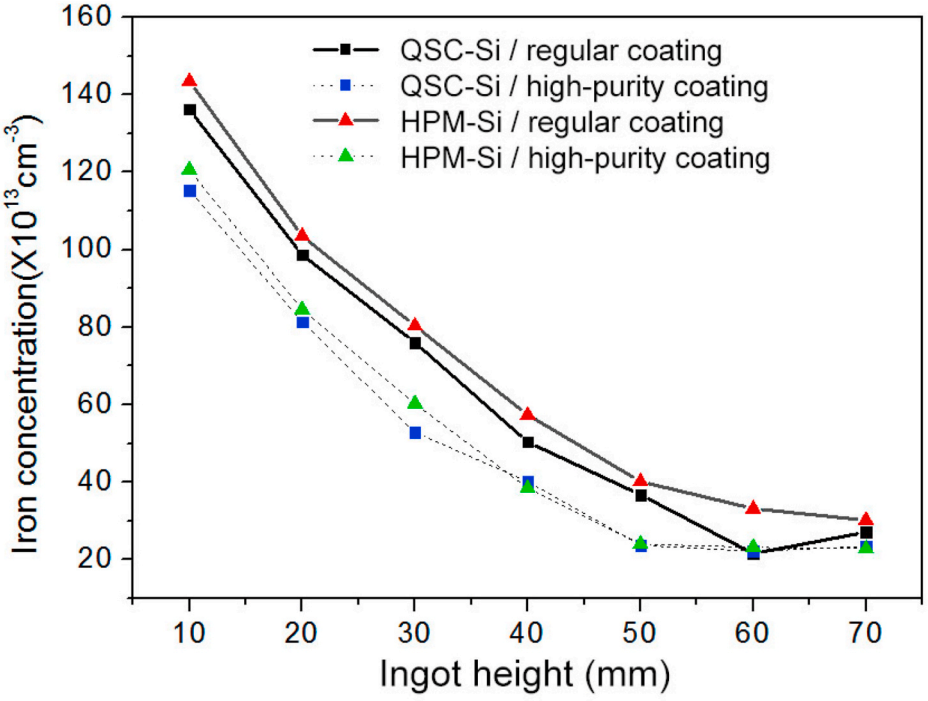


**Fig. 3.** Iron concentration distribution at the bottom of HPM-Si and QSC-Si ingots with regular or high-purity coating.

ingot is lower. It was also found that the concentration of interstitial oxygen decreases rapidly near the bottom of the Si ingot. At the edge of the red zone, the concentration of interstitial oxygen is nearly equal to the solubility of oxygen. Thus, oxygen precipitation is negligibly low, and the minority carrier lifetime increases rapidly.

## 4. Conclusions

The mechanism underlying the formation of the bottom red zone (i.e., the area where the minority carrier lifetime is less than 2 μs) at the bottom of cast ingots of quasi single crystalline Si was investigated in this study. It was found that metal and oxygen impurities were both responsible for the formation of bottom red zone. Saturated interstitial oxygen might form the precipitates and reduce the minority carrier lifetime at ingot bottom even with relatively low metal content. Thus, both the interstitial oxygen concentration and the metal concentration can determine bottom red zone height of industrial casting silicon ingots.

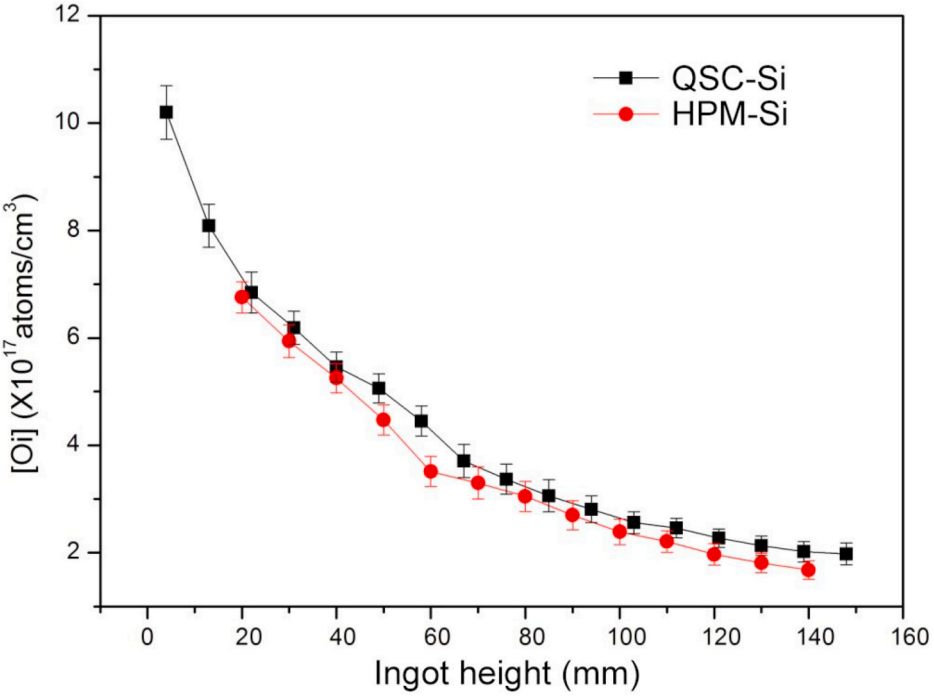


**Fig. 4.** Concentration of interstitial oxygen as a function of the distance from the bottom of the QSC-Si and HPM-Si ingots.

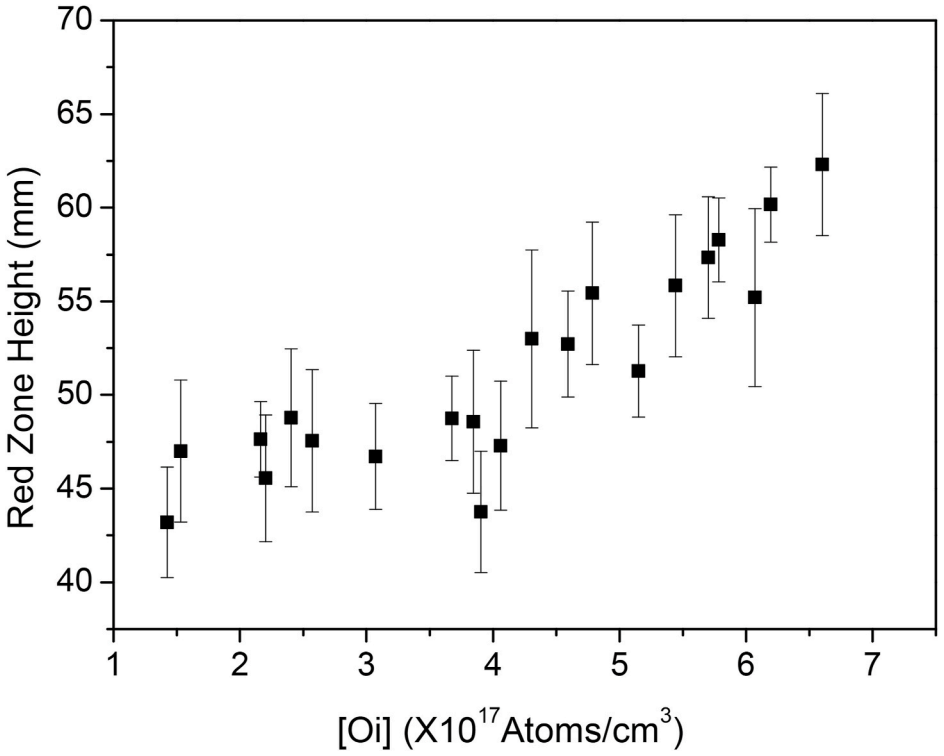


**Fig. 5.** Relationship of the interstitial oxygen content (at 45 mm height) and the QSC-Si red zone height.

## Authors' contributions

Chunlai Huang: Resources, Investigation, Data curation, Writing-Original draft preparation. Peng Wu: Visualization. Lei Wang: Conceptualization, Methodology, Writing- Reviewing and Editing. Deren Yang: Writing-Reviewing and Editing.

## Declaration of competing interest

The authors declare that they have no known competing financial interests or personal relationships that could have appeared to influence the work reported in this paper.

## Acknowledgements

This work was supported by the National Natural Science Foundation of China (No. 51532007, 61721005), National Key R&D Program of China (No. 2018YFB1500300), and Key Project of Zhejiang Province (No. 2018C01034).

## References

[1] G. Muller, J. Friedrich, Optimization and modeling of photovoltaic silicon crystallization processes, in: AIP Conference Proceedings 1270, 2010, pp. 255–281, 1.
[2] X. Gu, X. Yu, K. Guo, L. Chen, D. Wang, D. Yang, Seed-assisted cast quasi-single crystalline silicon for photovoltaic application: toward high efficiency and low cost silicon solar cells, Sol. Energy Mater. Sol. Cell. 101 (2012) 95–101.
[3] N. Stoddard, B. Wu, I. Witting, M. Wagener, Y. Park, G. Rozgonyi, R. Clark, Casting single crystal silicon: novel defect profiles from BP Solar's mono2 TM wafers, Solid State Phenom. 131 (2008) 1–8.
[4] N. Stoddard, R. Sidhu, G. Rozgonyi, I. Witting, P.V. Dollen, Monocrystalline Cast Silicon: a Present and Future Technology, International Workshop on Crystalline Silicon Solar Cells, 2009. Trondheim, Norway.
[5] D. Macdonald, A. Cuevas, A. Kinomura, Y. Nakano, L. Geerligs, Transition-metal profiles in a multicrystalline silicon ingot, J. Appl. Phys. 97 (2005), 033523.
[6] L. Liu, S. Nakano, K. Kakimoto, Dynamic simulation of temperature and iron distributions in a casting process for crystalline silicon solar cells with a global model, J. Cryst. Growth 292 (2006) 515–518.
[7] J.D. Murphy, K. Bothe, M. Olmo, V.V. Voronkov, R.J. Falster, The effect of oxide precipitates on minority carrier lifetime in p-type silicon, J. Appl. Phys. 110 (2011), 053713.
[8] T.U. Nærland, L. Arnberg, A. Holt, Origin of the low carrier lifetime edge zone in multicrystalline PV silicon, Prog. Photovoltaics Res. Appl. 17 (2009) 289–296.
[9] G. Zhong, Q. Yu, X. Huang, L. Liu, Influencing factors on the formation of the low minority carrier lifetime zone at the bottom of seed-assisted cast ingots, J. Cryst. Growth 402 (2014) 65–70.
[10] B. Gao, S. Nakano, K. Kakimoto, Influence of back-diffusion of iron impurity on lifetime distribution near the seed-crystal interface in seed cast-grown monocrystalline silicon by numerical modeling, Cryst. Growth Des. 12 (1) (2012) 522–525.
[11] X. Yu, X. Gu, S. Yuan, K. Guo, D. Yang, Two-peak characteristic distribution of iron impurities at the bottom of cast quasi-single-crystalline silicon ingot, Scripta Mater. 68 (2013) 655–657.
[12] F.M. Livinton, S. Messoloras, R.C. Newman, B.C. Pike, R.J. Stewart, M.J. Binns, W. P. Brown, J.G. Wilkes, An infrared and neutron scattering analysis of the precipitation of oxygen in dislocation-free silicon, J. Phys. C Solid State Phys. 17 (1985) 6253–6276.
[13] A. Borghesi, B. Pivac, A. Sassella, A. Stella, Oxygen precipitation in silicon, J. Appl. Phys. 77 (9) (1995) 4169–4244.